Oxy-Fuel Combustion for CO_2 Capture using a CO_2-Tolerant Oxygen Transporting Membrane

Yanying Wei, Yanjie Wang, Jun Tang, Zhong Li, and Haihui Wang
Key Laboratory of Enhanced Heat Transfer and Energy Conservation of the Ministry of Education, School of Chemistry and Chemical Engineering, South China University of Technology, 510640 Guangzhou, China

DOI 10.1002/aic.14131
Published online May 16, 2013 in Wiley Online Library (wileyonlinelibrary.com)

CO_2 capture via an oxy-fuel route through the U-shaped $(Pr_{0.9}La_{0.1})_2(Ni_{0.74}Cu_{0.21}Ga_{0.05})O_{4+\delta}$ (PLNCG) hollow fiber membrane with 100% CH_4 conversion and 100% CO_2 selectivity for 450 h has been explored for the first time. X-ray diffraction, scanning electron microscopy, and energy dispersive spectroscopy characterizations of the spent hollow fiber membrane have also been investigated. All these results indicate that PLNCG hollow fiber membrane shows excellent reaction performance and good stability under oxy-fuel reaction conditions, which will be a potential rounte for reducing CO_2 emissions worldwide. © 2013 American Institute of Chemical Engineers *AIChE J*, 59: 3856–3862, 2013
Keywords: membrane separations, oxygen permeation, hollow fiber, CO_2, oxy-fuel

Introduction

Environmental issues due to the emission of pollutants from fossil fuels combustion have become global problem. Combustion of fossil fuels leads to the CO_2 emission into the atmosphere, which is believed to contribute the undesired global problem.[1–4] Therefore, the reducing the emissions of CO_2 into the atmosphere became an urgent issue. Recently, CO_2 capture, storage, as well as the utilization technologies for reducing the CO_2 emission from fossil fuel fired power plants have gained great attention of academia, industry, and the decision makers in governments. Precombustion, oxy-fuel combustion, and post combustion are three major CO_2 capture technologies for power generation.[5] In the precombustion, the technique is complex and the total capital costs of the generating facility are very high, and the separation efficiency of H_2 and CO_2 also needs to be improved.[6] In the post combustion technology, the low concentration of CO_2 in the power-plant flue gas (typically 4–14%) means that a large volume of gas has to be handled, which results in a large equipment size and high capital costs. An attractive process is oxy-fuel combustion, that is, burning coal with pure O_2 or O_2/CO_2 mixtures instead of with air. There are several big projects around the world including CS Callide (Australia), Vattenfal (Germany), Inabensa (Spain), and the oxy-fuel coal combustion is the process of choice for the rejuvenated FutureGen (USA) program.[7] The oxy-fuel combustion concept for power generation relies on the idea that when the fossil fuel is combusted with oxygen, it generates a flue gas of mainly CO_2 and water, as well as small amounts of ash and trace elements. By cooling the flue gas, water can be easily removed and then the highly concentrated CO_2 can be easily obtained. To control the flame temperature and keep up the gas volume in the boiler,[8,9] the recycled CO_2 from the flue gas is normally used to dilute the oxygen before combustion. In this process, highly concentrated CO_2 can be produced for subsequent transportation and geological storage. However, the key problem is how to get cheap oxygen in a large scale for the oxy-fuel combustion.

Nowadays, there are two traditional ways to get pure oxygen in industry, that is, swing adsorption technology and cryogenic fractionation technology. Swing adsorption technology is mainly dominated by the large gas separation companies including BOC, Praxair, Air Products and Chemicals, Air Liquide, Linde, and UOP. However, the market for this mature technology is mainly in the small to medium range while large-scale is generally carried out by cryogenic separation processes. Cryogenic air separation is the most established technique for the large-scale production of O_2. However, the operation of the unit will consume about 15% of the electrical output of the power station.[10,11]

Another technology with potential air separation technology is dense ceramic membranes. These mixed ionic and electronic conducting (MIEC) membranes, which exhibit both ionic and electronic conducting properties to separate O_2 from air,[12] have attracted a large research effort in the last two decades. Of particular attention, integrating dense ceramic membranes in coal power generation can reduce O_2 energy costs by 35% or more as compared to conventional oxygen processes.[8,13,14] A key issue refers to CO_2 which causes instability of MIEC materials structure. Therefore, the development of CO_2-stable MIEC membrane material is very important for this concept. However, many alkaline-earth metal-containing materials are quite sensitive to CO_2 due to the formation of carbonates[15–21] and the oxygen permeation fluxes through these membranes usually decreases sharply once contacted with CO_2. In recent years, K_2NiF_4-type MIEC membrane materials, which are alkaline-earth metal-free, have been

Correspondence concerning this article should be addressed to H.H. Wang at hhwang@scut.edu.cn.

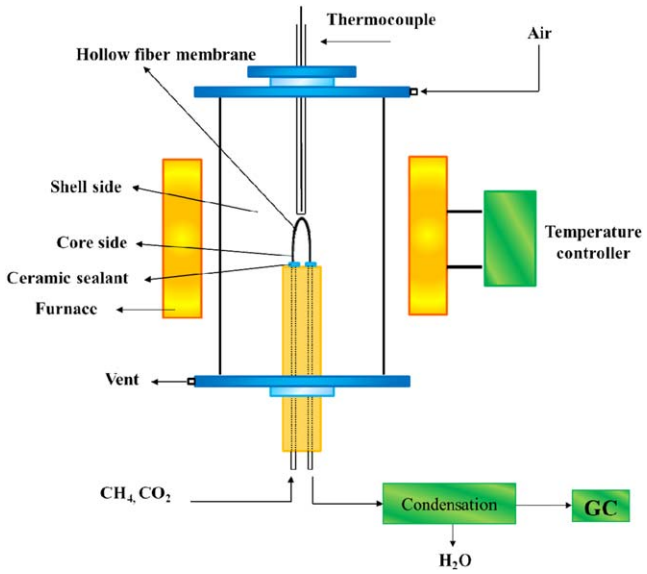

Figure 1. High-temperature membrane reactor for oxy-fuel combustion.

[Color figure can be viewed in the online issue, which is available at wileyonlinelibrary.com]

proved to be CO_2-tolerent, such as $La_2NiO_{4+\delta}$.[22,23] $(Pr_{0.9}La_{0.1})_2(Ni_{0.74}Cu_{0.21}Ga_{0.05})O_{4+\delta}$ (PLNCG) exhibits relatively high oxygen permeation rate, which is developed by Yashima et al.[24,25] Herein, we explored the CO_2 capture for power station based on the oxy-fuel combustion using a MIEC membrane, and PLNCG was chosen as the membrane reactor material due to its excellent stability and oxygen permeation under CO_2 from our previous work.[26,27]

Experimental

PLNCG powder was prepared through the sol-gel route with citric acid and ethylene diamine tetraacetic acid (EDTA).[26] The U-shaped[28] PLNCG hollow fiber membranes were prepared by phase-inversion spinning followed by sintering.[7,29–36] Details can be found in our previous work.[26,27]

The oxy-fuel combustion of methane in the U-shaped PLNCG hollow fiber membrane reactor was investigated in a high-temperature permeation cell, as shown in Figure 1. A mixture of CH_4 and CO_2 was fed to the core side while the air was fed to the shell side of the hollow fiber membrane. An online gas chromatograph (Agilent 7890) with a thermal conductivity detector was used to analyze the composition of the flue gas. The CH_4 conversion (X_{CH4}) and the CO_2 selectivity (S_{CO2}) are calculated as follows

$$X_{CH_4} = \left(1 - \frac{F_{CH_4}^{out}}{F_{CH_4}^{in}}\right) \times 100\% \quad (1)$$

$$S_{CO_2} = \left(1 - \frac{F_{CO}}{F_{CH_4}^{in} - F_{CH_4}^{out}}\right) \times 100\% \quad (2)$$

where F_{gas} is the flow rate of the corresponding gas.

The phase structures of the powder and sintered membranes were determined by x-ray diffraction (XRD, Bruker-D8 ADVANCE, Cu Kα radiation). The microstructures and the elemental compositions of the membranes were observed and analyzed by a scanning electron microscope (SEM, JEOL JSM-6490LA) and the energy dispersive spectroscopy (EDS).

Results and Discussion

Oxy-fuel combustion concept

The basic concept of oxy-fuel combustion for CO_2 capture based on the MIEC membranes is shown in Figure 2. At high temperatures, oxygen is transported through the MIEC hollow fiber membrane as oxygen ion. Simultaneously, electrons are transported in the opposite direction to maintain electric neutrality. Oxygen separated from the shell side of the hollow fiber is consumed in the core side by the methane combustion according to

$$CH_4 + 2O_2 \rightarrow CO_2 + 2H_2O \quad (3)$$

Thereby, the combustion process generates a flue gas consisting mainly of CO_2 and H_2O. After a simple downstream condensation of H_2O, then CO_2 can be easily removed. The recycled CO_2 replaces the N_2 in the combustion air to lower the flame temperature and keep the gas volume in the boiler.[8] The advantage of this combustion is that 100% CO_2 can be captured easily after condensation, which is helpful to realize the zero-emission power plant and beneficial to cut the cost of CO_2 capture.

Effect of different conditions on reaction performance

Figure 3 shows the effect of the temperature on the CH_4 conversion, CO_2 selectivity, and the oxygen permeation flux in the oxy-fuel combustion of methane in the U-shaped PLNCG hollow fiber membrane reactor. The oxygen permeation flux obviously increases with rising temperature because both of the oxygen surface exchange and the bulk diffusion are improved at high temperatures. As expected, the CH_4 conversion also increases with rising temperature due to the increase of the oxygen permeation flux, and it can even reach 100% at 975°C. However, the CO_2 selectivity decreases with increasing temperature when the temperature is below 925°C, whereas increases with increasing temperature when the temperature is above 950°C. Under the given conditions, the partial oxidation of methane as well as the total oxidation of methane simultaneously occur in the U-shaped PLNCG hollow fiber membrane reactor. In other words, both the reactions in Eqs. 3 and 4

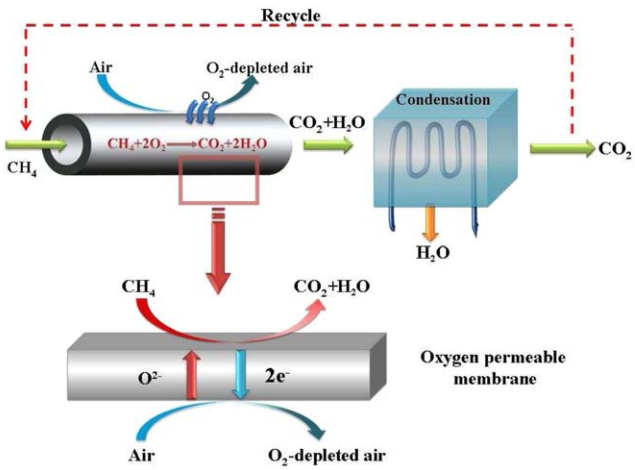

Figure 2. Concept of oxy-fuel combustion for CO_2 capture based on the MIEC membranes.

[Color figure can be viewed in the online issue, which is available at wileyonlinelibrary.com]

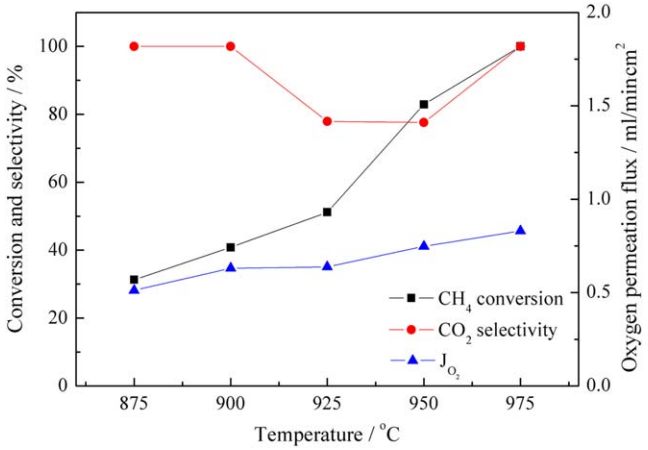

Figure 3. Effect of the temperature on the CH_4 conversion, CO_2 selectivity, and the oxygen permeation flux in the oxy-fuel combustion of methane.

Conditions: $F_{air} = 150$ mL/min, $F_{CH4+CO2} = 5.34$ mL/min, $C_{CH4} = 10\%$. [Color figure can be viewed in the online issue, which is available at wileyonlinelibrary.com]

$$CH_4 + \frac{1}{2}O_2 \rightarrow CO + 2H_2 \quad (4)$$

occur in the membrane reactor. The ratio of CH_4 to O_2 decreases with increasing temperature due to the increase of the oxygen permeation flux. Therefore, the partial oxidation of methane is the main reaction at lower temperatures, while the total oxidation of methane is the dominate reaction at higher temperatures. When the temperature is below 925°C, the amount of CO produced according to the partial oxidation increases with the increase of temperature, which leads to the decrease of the CO_2 selectivity as shown in Figure 3. On the other hand, when the temperature is above 950°C, the amount of CO_2 coming from the total oxidation of methane increases with increasing temperature, which results in the increase of CO_2 selectivity.

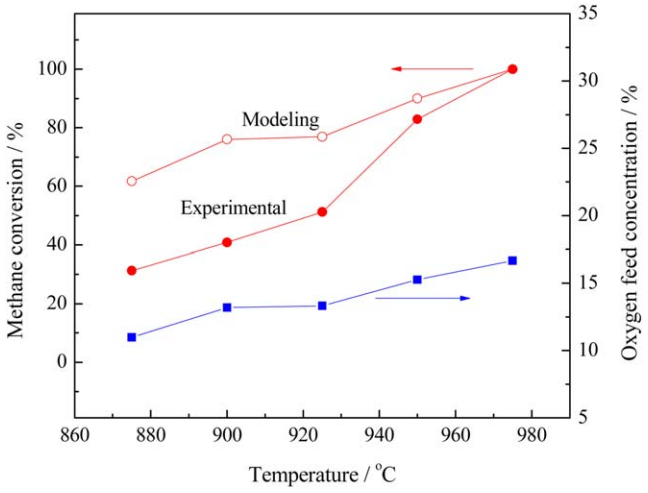

Figure 4. Dependence of methane conversion on temperature with different oxygen feed concentrations.

Solid: experimental results; open: modeling results. [Color figure can be viewed in the online issue, which is available at wileyonlinelibrary.com]

The methane conversion vs. temperature at different fed oxygen concentrations is calculated, as shown in Figure 4. The fed oxygen concentration increases with increasing temperature, which can be come from the enhanced oxygen permeation flux through the membrane. The simulated result of methane conversion increases from 61 to 100% during 875–975°C, whereas the experimental value increases from 31 to 100%. It has to be admitted that there is a difference between the modeling and experimental results, especially at relatively low temperatures. There are several reasons: (1) the hollow fiber membrane reactor with small inner diameter (about 500 μm) is regarded as a fixed-bed reactor with cm-scale dimension, which will bring in some difference between the microcosmic and macroscopical reactors; (2) the permeated oxygen through the membrane is distributed and the feed oxygen concentration varies along the hollow fiber membrane. However, for modeling, the oxygen concentration is assumed as a constant at each temperature. Actually, near the methane inlet, the ratio of CH_4/O_2 is relatively high and the oxygen can be consumed totally. Along the gas flow direction, the ratio of CH_4/O_2 decreases gradually. To the contrary, the ratio of CH_4/O_2 is relatively low and the oxygen cannot be consumed in time near the outlet. That is why the actual methane conversion is much lower than the modeling result; (3) the modeling results are calculated on the basis of ideal thermodynamic equilibrium and the reaction time is infinite. However, the simulated results are in good agreement with the experimental results at relatively high temperatures. It is because the reaction velocity increases with increasing temperature and the experimental results tend to achieve the simulated value.

Figure 5 shows the effect of the CH_4 concentration in the feed gas on the CH_4 conversion, the CO_2 selectivity, and the oxygen permeation flux in the oxy-fuel combustion of methane at 975°C. Different CH_4 concentrations are adjusted by changing the flow rate of the diluted gas (CO_2). In the CH_4 concentration range of 4.7–10%, CH_4 can be completely consumed by oxygen, and the CH_4 conversion is 100%. When the CH_4 concentration is below 7.6%, the CO_2 selectivity is 100%. However, when the CH_4 concentration is

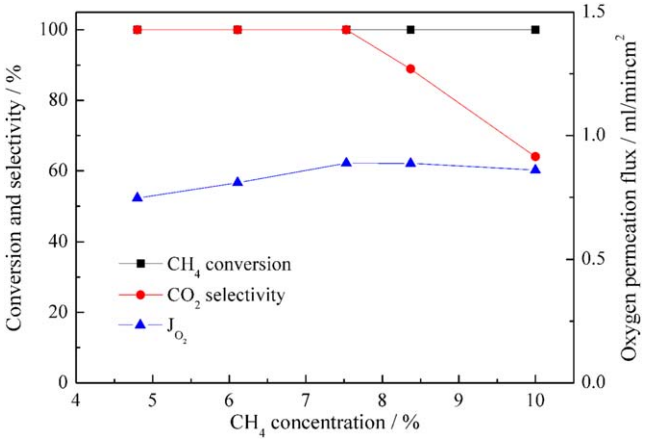

Figure 5. Effect of the CH_4 concentration in the sweep gas on the CH_4 conversion, CO_2 selectivity, and the oxygen permeation flux in the oxy-fuel combustion of methane at 975°C.

Conditions: $F_{air} = 150$ mL/min, $F_{CH4+CO2} = 7.33$ mL/min. [Color figure can be viewed in the online issue, which is available at wileyonlinelibrary.com]

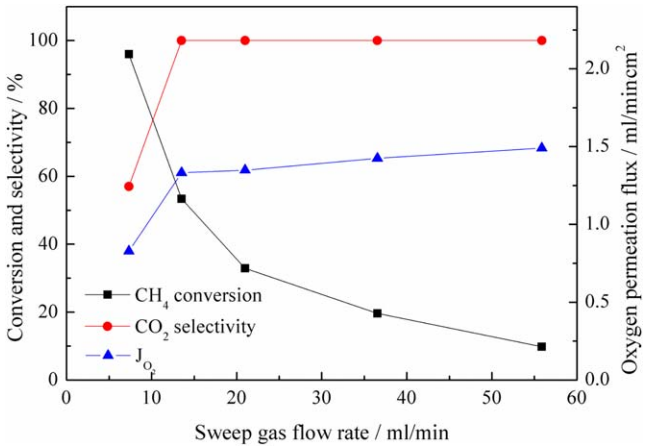

Figure 6. Effect of the high sweep gas flow rate on the CH_4 conversion, CO_2 selectivity, and the oxygen permeation flux in the oxy-fuel combustion of methane at 975°C.

Conditions: $F_{air} = 150$ mL/min, $F_{CH4} = 0.733$ mL/min. [Color figure can be viewed in the online issue, which is available at wileyonlinelibrary.com]

above 7.6%, the partial oxidation of methane also takes place in the hollow fiber membrane reactor, which causes the decrease of the CO_2 selectivity.

The effect of the flow rate in the core side on the CH_4 conversion, the CO_2 selectivity, and the oxygen permeation flux in the oxy-fuel combustion of methane at 975°C are presented in Figures 6 (high flow rate) and 7 (low flow rate). In both the two figures, the oxygen permeation flux increases with rising the total gas flow rate in the core side due to the increase of the oxygen permeation driving force. The CO_2 selectivity also increases with the increase of the oxygen permeation flux (shown in Figure 6), and it keeps 100% when the total gas flow rate in the core side is above 14 mL/min. However, the CH_4 conversion decreases with rising the total gas flow rate in the core side. As shown in Figure 7, CH_4 conversion keeps 100% due to the relatively low total gas flow rate in the core side and the long contact time with the membrane. At a constant CH_4 concentration of 10%, the CO_2 selectivity is 100% when the total gas flow rate in the core side is below 5.3 mL/min, whereas it decreases at higher total gas flow rate in the core side (>5.3 mL/min) which is due to the competition of the partial oxidation of methane.

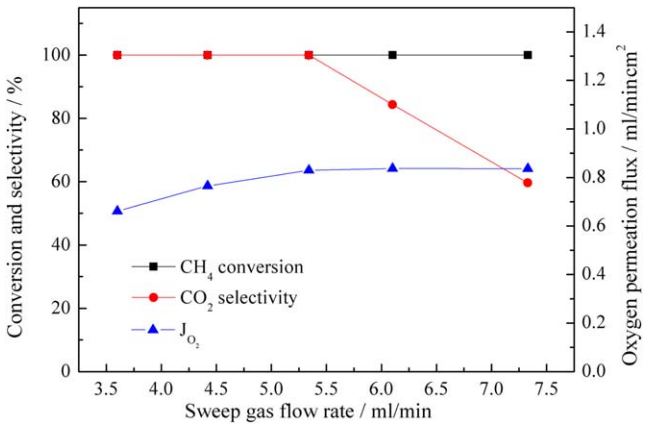

Figure 7. Effect of the low sweep gas flow rate on the CH_4 conversion, CO_2 selectivity, and the oxygen permeation flux in the oxy-fuel combustion of methane at 975°C.

Conditions: $F_{air} = 150$ mL/min, $C_{CH4} = 10\%$. [Color figure can be viewed in the online issue, which is available at wileyonlinelibrary.com]

Long-term performance

It has been reached a consensus that the oxygen permeable membranes-based oxy-fuel technology is likely to become an economically justified technology which is able to push forward the carbon capture and storage and particular the oxy-fuel technology to commercial realization.[37] However, it has to be pointed out that the oxy-fuel combustion with flue gas recycling has not been carried out on a pilot scale because none of the presently known oxygen permeable membrane materials with appreciable oxygen fluxes were found to be stable under the harsh conditions of a real flue gas (CO_2, SO_2, ash, etc.).[37,38] Therefore, it is still a challenge to apply the oxygen permeable membranes in oxy-fuel technology with CO_2 capture. A key issue refers to CO_2 which causes instability of MIEC materials structure. In other words, the CO_2-stable MIEC membrane material is very necessary for this concept. In our previous work, PLNCG has been proved to be CO_2-tolerant.[26,27] During an 310-h oxygen permeation test, the oxygen permeation flux keeps constant even though CO_2 exists simultaneously on the both air and sweep sides of the PLNCG hollow fiber membrane, which indicates the excellent stability of PLNCG under CO_2-containing atmosphere.[27] Therefore, PLNCG can be expect to be applied to supply oxygen for the oxy-fuel combustion with CO_2 capture for long-term operation.

As expected, the U-shaped PLNCG hollow fiber membrane exhibits excellent stability when it is applied in the oxy-fuel combustion of methane. Figure 8 shows the long-term behaviors of the CH_4 conversion, the CO_2 selectivity, and the oxygen permeation flux in the oxy-fuel combustion in the U-shaped PLNCG hollow fiber membrane reactor at 975°C. During this combustion test, 100% CH_4 conversion with 100% CO_2 selectivity are obtained steadily. It should be noted that a mixture of 90% CO_2 with 10% CH_4 was fed

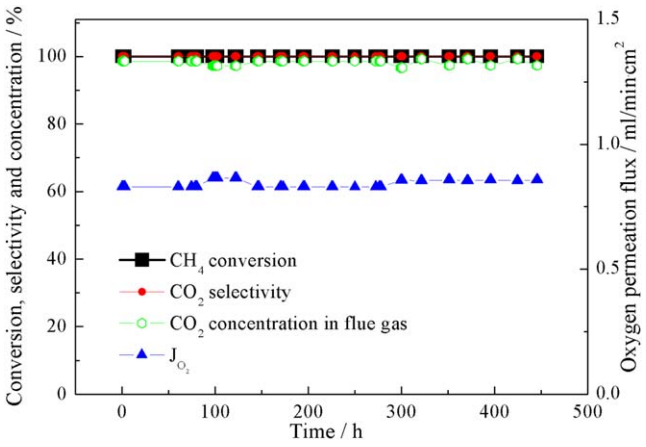

Figure 8. Long-term operation of the oxy-fuel combustion of methane in the U-shaped PLNCG hollow fiber membrane reactor at 975°C.

Conditions: $F_{air} = 150$ mL/min, $F_{CH4+CO2} = 5.34$ mL/min, $C_{CH4} = 10\%$. [Color figure can be viewed in the online issue, which is available at wileyonlinelibrary.com]

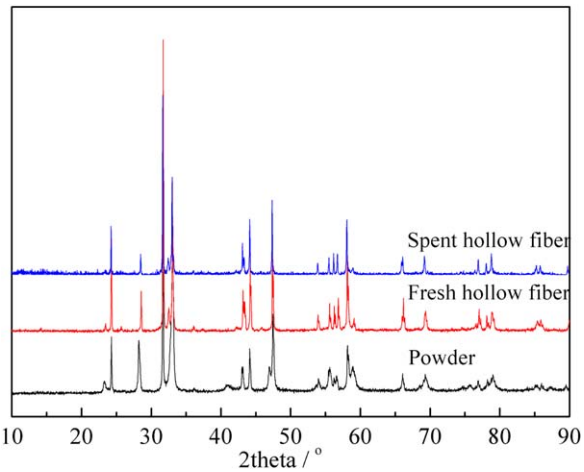

Figure 9. XRD patterns of the PLNCG powder, fresh, and spent hollow fiber membrane after 450-h operation of methane combustion (in Figure 8).

[Color figure can be viewed in the online issue, which is available at wileyonlinelibrary.com]

to the core side in our long-term operation experiment and no inert gas was used here for dilution. The CO_2 concentration in the flue gas of this oxy-fuel combustion system is above 96%. Comparing to the methane combustion with He dilution in the $La_{0.6}Sr_{0.4}Co_{0.2}Fe_{0.8}O_{3-\delta}$ membrane reactor,[39] the results of oxy-fuel combustion of methane in such a K_2NiF_4-type oxide membrane reactor indicate a better reaction performance. The oxygen permeation flux through such a U-shaped PLNCG hollow fiber membrane in this oxy-fuel combustion process keeps around 0.85 mL/min cm^2. During the 450-h operation, the CH_4 conversion, the CO_2 selectivity, and the oxygen permeation flux are steady and no decrease is found, which shows a good stability of this membrane. It should be pointed out that although we had to stop the test, the U-shaped PLNCG hollow fiber is still gas-tight after 450 h.

Characterization of the spent membrane

After the long-term oxy-fuel combustion, the spent PLNCG hollow fiber membrane is characterized by XRD, SEM, and EDS. Figure 9 presents the phase structures of the PLNCG powder prepared by a combined EDTA-citrate complexation, the fresh hollow fiber membrane sintered at 1300°C, and the spent hollow fiber membrane after 450-h oxy-fuel combustion with high concentration of CO_2 (in Figure 8). The XRD patterns indicate all of them are pure K_2NiF_4 structure. Furthermore, after the 450-h oxy-fuel combustion, no carbonate is observed which indicates that the U-shaped PLNCG hollow fiber membrane exhibits excellent phase structure stability in the flue gas atmosphere of the oxy-fuel combustion.

Figure 10 also shows the SEM micrographs of the fresh and spent PLNCG hollow fiber membrane after 450 h oxy-fuel combustion. Figures 10A, B show the top view and the wall of the fresh PLNCG hollow fiber membrane. An asymmetry structure with a porous inner layer and a dense outer layer can be observed on the membrane wall, which is beneficial to the oxygen permeation. Actually, such an asymmetry structure was formed during the phase-inversion process in one step. In other words, the formation of the porous and dense structures is resulted from the different diffusion speed of solvent and nonsolvent in the phase-inversion process.[40]

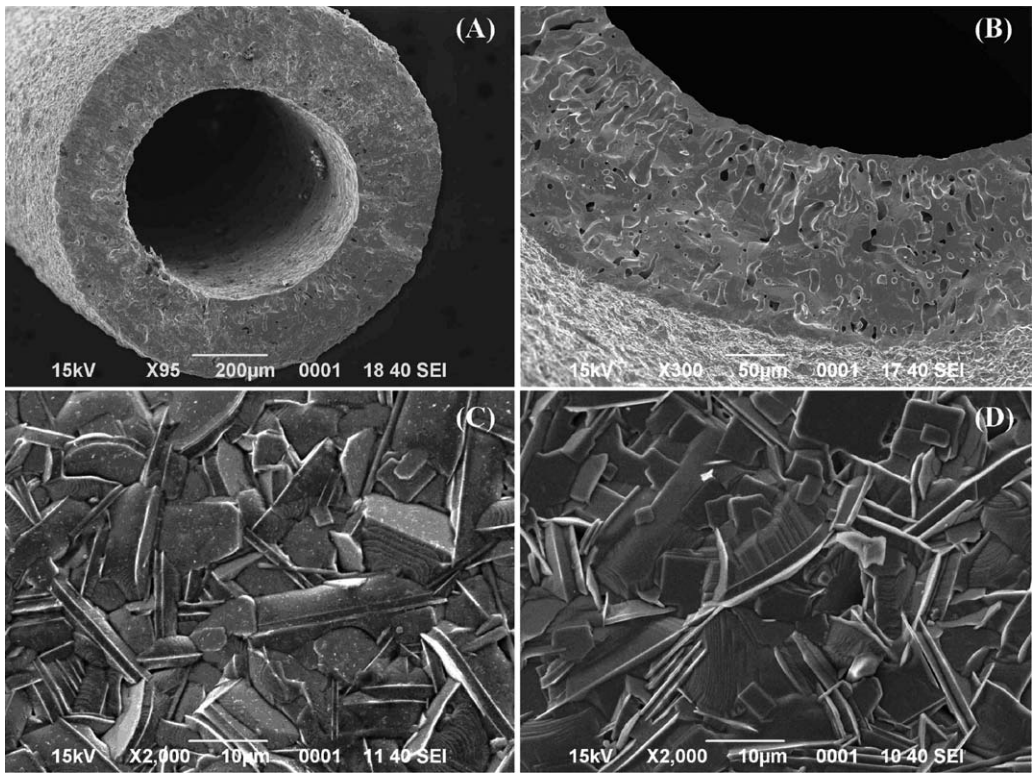

Figure 10. SEM micrographs of the PLNCG hollow fiber membrane.

(A) top view, (B) the wall of the fresh hollow fiber, (C) inner surface of the fresh, and (D) spent hollow fiber after 450-h operation of methane combustion (in Figure 8).

Near the outer surface, the solvent flux is higher than the nonsolvent flux, thus, the polymer concentration at the outer surface would increase and it is contrary to the inner surface. That is why the asymmetry structure can be formed in one step during phase-inversion. Figures 10C, D present the inner surfaces of the fresh and spent PLNCG hollow fiber membrane after 450-h oxy-fuel combustion with high concentration of CO_2 (in Figure 8). The particles on the inner surfaces of both the fresh and spent membrane connect to each other firmly. After the long-term oxy-fuel combustion, the inner surface close to the reaction side of spent hollow fiber membrane keeps intact which is similar to the fresh one (Figure 10C) and no carbon was detected by EDS, which indicates the good stability under the harsh oxy-fuel combustion conditions.

Conclusion

In summary, the CO_2 capture for power station based on the oxy-fuel combustion using a novel MIEC membrane of the composition PLNCG in hollow fiber geometry is explored. During the 450-h operation, 100% CH_4 conversion and 100% CO_2 selectivity are obtained steadily, which shows an excellent reaction performance. XRD, SEM, and EDS characterizations indicate that the spent membrane still maintains the perfect K_2NiF_4-type phase structure and intact microstructure without carbonate. To the best of our knowledge, this is the first report on the oxy-fuel combustion of methane in a ceramic hollow fiber membrane reactor using the recycled CO_2 diluted methane as the feed gas without inert gas for dilution. The oxygen permeable membrane-based oxy-fuel technology of fossil fuel is still in its early stages, and more laboratory efforts should be given in the near future.

Acknowledgment

The authors greatly acknowledge the financial support by National Science Fund for Distinguished Young Scholars of China (no. 21225625), Natural Science Foundation of China (nos. 21176087, 20936001), and the Pearl River Scholar Program of Guangdong Province.

Literature Cited

1. Neftel A, Moor E, Oeschger H, Stauffer B. Evidence from polar ice cores for the increase in atmospheric CO2 in the past two centuries. *Nature*. 1985;315:45–47.
2. Tans P. NOAA/ESRL. Trends in atmospheric carbon dioxide; available at http://www.esrl.noaa.gov/gmd/ccgg/trends/mlo.html.
3. Keeling RF, Piper SC, Bollenbacher AF, Walker JS. Atmospheric CO_2 Records from Sites in the SIO Sampling Network. In Trends: A Compendium of Data on Global Change, Oak Ridge, TN: Carbon Dioxide Information Analyses Center, Oak Ridge National Laboratory, US Department of Energy, 2009. doi: 10.3334/CDIAC/atg.035.
4. International Energy Agency. Key World Energy Statistics, 2008; available at http://iklim.cob.gov.tr/iklim/Files/eKutuphane/Key%20world%20Energy%20Statistics.pdf.
5. Irons R, Sekkapan G, Panesar R, Gibbins J, Lucqiuaud M. CO_2 capture ready plants. Prepared for IEA greenhouse gas R&D programme. available at http://www.iea.org/publications/freepublications/publication/CO2_Capture_Ready_Plants.pdf.
6. Olajire AA. CO2 capture and separation technilogies for end-of-pipe applications. *Energy*. 2010;35:2610–2628.
7. Sunarso J, Liu S, Lin YS, da Costa JCD. High performance BaBiScCo hollow fibre membranes for oxygen transport. *Energy Environ Sci*. 2011;4:2516–2519.
8. Buhre BJP, Elliot LK, Sheng CD, Gupta RP, Wall TF. Oxy-fuel combustion technology for coal-fired power generation. *Prog Energy Combust Sci*. 2005;31:283–307.
9. Glaarborg P, Bentzen LB. Chemical effects of a high CO2 concentration in oxy-fuel combustion of methane. *Energy Fuels*. 2008;22:291–296.
10. Andersson K, Maksinen P. Process Evaluation of CO_2 Free Combustion in an O_2/CO_2 Power Plant. Master Thesis, Chalmers University of Technology, Sweden, 2002.
11. Armstrong P. Fogash K. The 2nd Workshop on International Oxy-combustion Research Network, Windsor, CT, 2007. Hosted by Alstom Power Inc.
12. Steven HP, Roger ADS, Manfred M. Diffusion of La and Mn in Ba0.5Sr0.5Co0.8Fe0.2O3-δ polycrystalline ceramics. *Energy Environ Sci*. 2012;5:5803–5813.
13. Ren JY, Fan YQ, Egolfopoulos FN, Tsotsis TT. Membrane-based reactive separations for power generation applications: oxygen lancing. *Chem Eng Sci*. 2003;58:1043–1052.
14. Fan YQ, Ren JY, Onstot W, Pasale J, Tsotsis TT, Egolfopoulos FN. Reactor and technical feasibility aspects of a CO2 decomposition-based power generation cycle, utilizing a high-temperature membrane reactor. *Ind Eng Chem Res*. 2003;42:2618–2626.
15. Arnold M, Wang HH, Feldhoff A. Influence of CO2 on the oxygen permeation performance and the microstructure of perovskite-type (Ba0.5Sr0.5)(Co0.8Fe0.2)O3-δ membranes. *J Membr Sci*. 2007;293:44–52.
16. Yi JX, Schroeder M, Weirich T, Mayer J. Behavior of Ba(Co, Fe, Nb)O3-δ perovskite in CO2-containing atmospheres: degradation mechanism and materials design. *Chem Mater*. 2010;22:6246–6253.
17. Czuprata O, Arnold M, Schirrmeister S, Schiestel T, Caro J. Influence of CO2 on the oxygen permeation performance of perovskite-type BaCoxFeyZrzO3-δhollow fiber membranes. *J Membr Sci*. 2010;364:132–137.
18. Martynczuk J, Efimov K, Robben L, Feldhoff A. Performance of zinc-doped perovskite-type membranes at intermediate temperatures for long-term oxygen permeation and under a carbon dioxide atmosphere. *J Membr Sci*. 2009;344:62–70.
19. Yang Q, Lin YS, Bulow M. High temperature sorption separation of air for producing oxygen-enriched CO2 stream. *AIChE J*. 2006;52:574–581.
20. Yi JX, Feng SJ, Zuo YB, Liu W, Chen CS. Oxygen permeability and stability of Sr0.95Co0.8Fe0.2O3-δ in a CO2- and H2O-containing atmosphere. *Chem Mater*. 2005;17:5856–5861.
21. Jin WQ, Zhang C, Zhang P, Fan YQ, Xu NP. Thermal decomposition of carbon dioxide coupled with POM in a membrane reactor. *AIChE J*. 2006;52:2545–2550.
22. Klande T, Efimov K, Cusenza S, Becker KD, Feldhoff A. Effect of doping, microstructure, and CO2 on La2NiO4+δ-based oxygen-transporting materials. *J. Solid State Chem*. 2011;184:3310–3318.
23. Engels S, Markus T, Modigell M, Singheiser L. Oxygen permeation and stability investigations on MIEC membrane materials under operating conditions for power plant processes. *J Membr Sci*. 2011;370:58–69.
24. Yashima M, Enoki M, Wakita T, Ali R, Matsushita Y, Izumi F, Ishihara T. Structural disorder and diffusional pathway of oxide ions in a doped Pr2NiO4-based mixed conductor. *J Am Chem Soc*. 2008;130:2762–2763.
25. Yashima M, Sirikanda N, Shihara T. Crystal structure, diffusion path, and oxygen permeability of a Pr2NiO4-based mixed conductor (Pr0.9La0.1)2(Ni0.74Cu0.21Ga0.05)O4+δ. *J Am Chem Soc*. 2010;132:2385–2392.
26. Tang J, Wei YY, Zhou LY, Li Z, Wang HH. Oxygen permeation through a CO2-tolerant mixed conducting oxide (Pr0.9La0.1)2(Ni0.74Cu0.21Ga0.05)O4+δ. *AIChE J*. 2012;58:2473–2478.
27. Wei YY, Tang J, Zhou LY, Xue J, Li Z, Wang HH. Oxygen separation through U-shaped hollow fiber membrane using pure CO2 as sweep gas. *AIChE J*. 2012;58:2856–2864.
28. Wei YY, Liu HF, Xue J, Li Z, Wang HH. Preparation and oxygen permeation of U-shaped perovskite hollow fiber membranes. *AIChE J*. 2011;57:975–984.
29. Liu SM, Gavalas GR. Preparation of oxygen ion conducting ceramic hollow-fiber membranes. *Ind Eng Chem Res*. 2005;44:7633–7637.
30. Tan XY, Liu Y, Li K. Mixed conducting ceramic hollow-fiber membranes for air separation. *AIChE J*. 2005;51:1991–2000.
31. Tan XY, Li K. Oxygen production using dense ceramic hollow fiber membrane modules with different operating modes. *AIChE J*. 2007;53:838–845.

32. Liu SM, Tan XY, Li K, Hughes R. Preparation and characterization of SrCe0.95Yb0.05O2.975 hollow fiber membranes. *J Membr Sci*. 2001;193:249–260.
33. Liu SM, Tan XY, Shao ZP, da Costa JCD. Ba0.5Sr0.5Co0.8-Fe0.2O3-δ. ceramic hollow-fiber membranes for oxygen permeation. *AIChE J*. 2006;52:3452–3461.
34. Schiestel T, Kilgus M, Peter S, Caspary KJ, Wang HH, Caro J. Hollow fibre perovskite membranes for oxygen separation. *J Membr Sci*. 2005;258:1–4.
35. Trunec M. Fabrication of zirconia- and ceria-based thin-wall tubes by thermoplastic extrusion. *J Eur Ceram Soc*. 2004;24:645–651.
36. Luyten J, Buekenhoudt A, Adriansens W, Cooymans J, Weyten H, Servaes F, Leysen R. Preparation of LaSrCoFeO3-x membranes. *Solid State Ionics*. 2000;135:637–642.
37. Stadler H, Beggel F, Habermehl M, Persigehl B, Kneer R, Modigell M, Jeschke P. Oxyfuel coal combustion by efficient integration of oxygen transport membranes. *Int J Greenh Gas Con*. 2011;5:7–15.
38. Czyperek M, Zapp P, Bouwmeester HJM, Modigell M, Ebert K, Voigt I, Meulenberg WA, Singheiser L, Stover D. Gas separation membranes for zero-emission fossil power plants: MEM-BRAIN. *J Membr Sci*. 2010;359:149–159.
39. Tan XY, Li K, Thursfield A, Metcalfe IS. Oxyfuel combustion using a catalytic ceramic membrane reactor. *Catal Today*. 2008;131:292–304.
40. Li K, Tan XY, Liu YT. Single-step fabrication of ceramic hollow fibers for oxygen permeation. *J Membr Sci*. 2006;272:1–5.

Manuscript received Sept. 5, 2012, and revision received Mar. 13, 2013.